


Speeding up nanomagnetic logic by DMI enhanced Pt/Co/Ir films

Special Collection: [62nd Annual Conference on Magnetism and Magnetic Materials](#)

Grazvydas Ziemys ; Valentin Ahrens; Simon Mendisch ; Gyorgy Csaba; Markus Becherer

 Check for updates

AIP Advances 8, 056310 (2018)

<https://doi.org/10.1063/1.5007308>



View
Online



Export
Citation

Articles You May Be Interested In

On the discrimination between nucleation and propagation in nanomagnetic logic devices

AIP Advances (December 2017)

Controlled data storage for non-volatile memory cells embedded in nano magnetic logic

AIP Advances (January 2017)

Experiment-based thermal micromagnetic simulations of the magnetization reversal for ns-range clocked nanomagnetic logic

AIP Advances (January 2017)

AIP Advances

Why Publish With Us?



19 DAYS
average time
to 1st decision



500+ VIEWS
per article (average)



INCLUSIVE
scope

[Learn More](#)



Speeding up nanomagnetic logic by DMI enhanced Pt/Co/Ir films

Grazvydas Ziemys,^{1,a} Valentin Ahrens,¹ Simon Mendisch,² Gyorgy Csaba,³ and Markus Becherer²

¹Chair of Circuit Design, Technical University of Munich (TUM), Germany

²Chair of Nanoelectronics, Technical University of Munich (TUM), Germany

³Faculty of Information Technology and Bionics Pázmány Péter Catholic University Budapest, Hungary

(Presented 7 November 2017; received 2 October 2017; accepted 2 November 2017; published online 19 December 2017)

We investigated a new type of multilayer film for Nanomagnetic Logic with perpendicular anisotropy (pNML) enhanced by the Dzyaloshinskii-Moriya interaction (DMI). The DMI effect provides an additional energy term and widens the design space for pNML film optimization. In this work we added an Ir layer between Co and Pt to our standard pNML multilayer (ML) film stack - [Co/Pt]_{x4}. Multilayer stacks of films with and w/o Ir were sputtered and patterned to nanowires of 400 nm width by means of focused ion beam lithography (FIB). For comparability of the films they were tuned to show identical anisotropy for multilayer stacks with and w/o Ir. The field-driven domain wall (DW) velocity in the nanowires was measured by using wide-field MOKE microscopy. We found a strong impact of Ir on the DW velocity being up to 2 times higher compared to the standard [Co/Pt]_{x4} ML films. Moreover, the maximum velocity is reached at much lower magnetic field, which is beneficial for pNML operation. These results pave the way for pNML with higher clocking rates and at the same time allow a further reduce power consumption. © 2017 Author(s). All article content, except where otherwise noted, is licensed under a Creative Commons Attribution (CC BY) license (<http://creativecommons.org/licenses/by/4.0/>). <https://doi.org/10.1063/1.5007308>

I. INTRODUCTION

Nanomagnetic Logic (NML) is one of the most mature and favorable candidates for the Beyond CMOS scaling era and is also listed in the latest International Technology Roadmap for Semiconductors 2015 (ITRS) in the “Beyond CMOS” technology Chapter.¹ NML offers several advantages over CMOS, nevertheless, NML is compatible with the existing CMOS processes, which allows hybrid CMOS/NML circuits on the same die, making use of the advantages of both technologies. First benchmarking against CMOS shows that NML consumes at least 35 times less energy for NAND/NOR operation compared to CMOS.² Moreover, stacking several functional layers of NML on top of each other allows high packing densities by employing monolithic 3D integration, as experimentally shown by Refs. 3 and 4. In addition, NML retains its current computational state, with no supplied energy, and thus comprises memory and logic functionality in a single technology.⁵ Those merits make NML very a attractive candidate for broad use cases: from ultra-low power computing in Internet of Things (IoT), implementation of co-processor or pattern matching hardware to high performance computing, such as massively parallel, deeply pipelined and high throughput data processing in big data applications.⁶ NML is one of the most competitive and experimentally proven candidates for the Beyond-CMOS devices research field. Due to inherent memory functionality in logic also new kinds of architectures such as in-memory computing can be explored.

^ag.ziemys@tum.de

There are two types of NML: one based on the in-plane (iNML), and second - on the out-of-plane (pNML) magnetization. The latter is more suitable for applications due to easier manufacturing processes. The functionality of iNML relies on precise form of nanomagnets, which is prone to fabrication shape errors. In contrast, direction of magnetization in pNML is defined by the magnetic multilayer materials and, therefore, this technology is more robust in terms of shape variation. This paper focuses on the NML with perpendicular magnetization.

pNML is based on bistable nanomagnets, which so far are made of Co/Pt or Co/Ni ultra thin multilayer films, but several other materials such a CoFeB, and Fe/Pt are envisioned for pNML. The logical states ('1' and '0') are encoded in the magnetization vector. Due to crystallinity and interface of Co/Pt or Co/Ni thin films, the magnetization vector has only two stable states pointing perpendicular to the surface plane of the magnet. By engineering the perpendicular magnetic anisotropy of such multilayer films it is ensured that all magnets have just a single magnetic domain in a steady state. Logic operations are carried out by magnetic field-coupled nanomagnets. The most basic pNML element is an inverter, which consists of two magnets placed near each other. Due to the fact that all systems try to minimize their energy, the magnetization vectors of these two magnets align anti-parallel to each other. Directionality of the signal is ensured by the generation of a weak spot on one side of a nanomagnet.⁷ This ensures that e.g. the magnet on the right is only sensitive to the one on the left side. The weak spot is called the artificial nucleation center (ANC) and is generated by irradiation of an area of typically 50x50nm with a focused ion beam (FIB), which locally reduces the magnetic anisotropy by intermixing the Co/Pt or Co/Ni layers and thus sensitizing the nanomagnet to the magnetic stray fields of the neighboring nanomagnets on one side.^{8,9} The key element of the nanomagnetic logic is the majority gate.¹⁰ It is a gate that has at least three inputs and one output. The output always aligns anti-parallel to the majority of the inputs. If one of the three inputs is fixed, the majority gate acts as NAND/NOR gate depending on the state of the fixed input. This allows to build an arbitrary logic function. To propagate the information through such gates an external alternating magnetic field is needed. The amplitude of such field is set in such a way that the magnets can only switch if the superposition of stray field of the neighboring magnet and the external field are constructive. This alternating field acts as a clock signal and it also provides the energy for the system. The clocking field is generated globally by an on-chip coil. An on-chip meander-like current conductor structure, embedded between a high μ_r material, such as Permalloy, is used to minimize the electrical current, needed to generate the clocking field.¹¹

To make pNML even more competitive candidate for the beyond-CMOS scaling era a higher clocking rate needs to be achieved. The biggest hindering factor for that is the domain wall propagation. A new domain is generated at the ANC, then it needs to be propagated along the whole magnet to induce the stray field on the subsequent neighboring magnet. Those two processes (nucleation and propagation) should happen during one half of the clocking cycle. Depending on the clocking field strength and multilayer film parameters (mainly damping constant) nucleation is reported to take less than fraction of a nanosecond.¹² In comparison, maximum domain wall speed in common pNML Co/Pt multilayer films saturates at around 40m/s, thus the time needed to propagate the new nucleated domain through the whole magnet takes several tens of nanoseconds. To address this issue we enhanced the standard $[\text{Co/Pt}]_{x4}$ pNML film stack by adding the Ir layer on top of each layer of Co. As reported in recent research, breaking the symmetry of Co interfaces by inserting a heavy metal with large spin orbit coupling results in strong antisymmetric exchange interaction called Dzyaloshinskii-Moriya interaction, which is supposed significantly support the domain wall motion.^{13,14}

II. FABRICATION AND EXPERIMENT

To explore the effect of iridium layer insertion in standard pNML $[\text{Co/Pt}]_{x4}$ multilayer, we deposited a following film stack: $\text{Ta}_2/\text{Pt}_3/\text{Co}_{0.75}/\text{Ir}_{0.38}[\text{Pt}_{0.94}\text{Co}_{0.75}/\text{Ir}_{0.36}]_{3x}/\text{Pt}_3$ (in nm) by magnetron sputtering (base pressure: 10^{-7} mBar, partial argon pressure 4 μ Bar). Then a standard pNML multilayer film $\text{Ta}_2/\text{Pt}_3/\text{Co}_{0.75}[\text{Pt}_{1.19}\text{Co}_{0.75}]_{3x}/\text{Pt}_3$ was fabricated and tuned by adjusting Pt layer to show the same value of effective anisotropy. Fig.1 shows laser-MOKE microscope images of the demagnetized samples. Although the measured effective anisotropy is almost identical, domain size

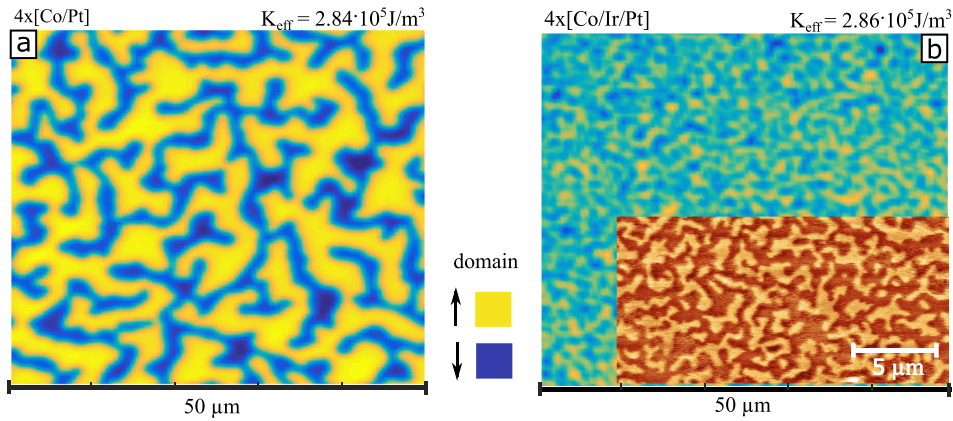


FIG. 1. Laser Kerr-effect microscope images of the demagnetized multilayer films right after sputter deposition. Blue and yellow colors indicating the magnetization direction. a) The image of the standard pNML multilayer stack shows relatively large domains, while the image of an iridium enhanced multilayer film stack (b) shows very small domains. To resolve the small domains of Ir enhanced sample, magnetic force microscope (MFM) image is shown in the inset b). Nevertheless, both films show nearly identical anisotropy, which was measured by extraordinary Hall-effect.

after demagnetization with the alternating external magnetic field perpendicular to the sample plane is drastically reduced in the sample with iridium (Fig. 1b)). The reason for that is the Dzyaloshinskii-Moriya interaction due to introduced iridium layers. We performed effective magnetic anisotropy measurements by evaluating the anomalous Hall-effect (AHE) voltage while rotating the sample in an external magnetic field. The AHE voltage is proportional to the perpendicular magnetization of the sample. By rotating the sample in the external homogenous magnetic field the magnetization vector deviates from external field vector depending on the effective magnetic anisotropy of the sample. Higher magnetic anisotropy leads to higher deviation and *vice versa*. Finally, fitting the resulting AHE voltage as described in Ref. 15 provides K_{eff} . The drawback of this measurement, however, is that the exact value of saturation magnetization (M_s) needs to be known. We have measured the M_s of Co/Pt ML films with various numbers of Co layers. This proved that it is legitimate to use a following equation for the M_s estimation with a measurement error of $\pm 9\%$:

$$M_s = \frac{N_{layers} \cdot M_{s,Co} \cdot t_{Co}}{N_{layers} \cdot t_{Co} + N_{layers} \cdot t_{Pt} + N_{layers} \cdot t_{Ir}} \quad (1)$$

By this, we treat the multilayer stack as effective media with reduced saturation magnetization M_s , averaged over the complete stack without seed. The AHE measurements averages over the whole multilayer, which consist of 8 layers. Only one half of them are magnetic and, therefore, the overall saturation magnetization is reduced when compared to the cobalt. Also the so-called proximity effect could be the reason of such relatively high error magnitude in M_s measurements. It is known that in particular Pt develops an induced moment in proximity to the Co layer.¹⁶ Significant reduction of the domain size was also observed in the samples with the same film stack except that in one of the iridium layers after each cobalt layer was introduced (Co and Pt layer thickness was kept constant in both samples). This result leads to the assumption that some additional energy, i.e. the DMI is introduced in a film by adding the Ir layers to Co/Pt ML system.

After the film characterization the magnetic nanowires of 400nm were structured in the film by focused ion beam lithography using positive e-beam resist - PMMA. A 750 nm thick Cu/Al conductor was patterned and aligned with the magnetic nanowires by photo-lithography and lift-off in order to apply short magnetic field pulses to the DUTs. Copper is chosen due to its conductivity and the top layer of 250nm aluminum is needed for wire-bonding of the sample on the chip-carrier, which contains the nanosecond pulse generator. The overview of the sample is presented in the Fig.2. To measure the velocity of a domain wall propagation in the magnetic nanowires with and w/o iridium layer, the wide field Kerr-effect microscope (WMOKE) was utilized. WMOKE allows spatially resolved evaluation of the magnetization of the nanowires. Firstly, the DW is nucleated at the ANC, which is

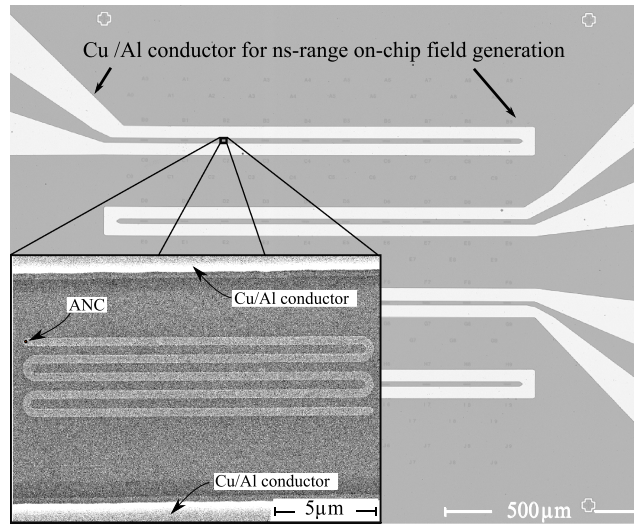


FIG. 2. Overview of the sample obtained by optical microscope. The white structures are Cu/Al on-chip coils. The meander like magnetic nanowires are embedded between two fingers of an on-chip coil, as shown in the SEM image in the inset.

generated by the FIB as described above. The ANC is placed at the beginning of a nanowire to enable more external magnetic field pulses until the whole nanowire is switched (see the inset in Fig.2). Then, the nanowires are saturated in one direction by applying high external field, perpendicular to the sample plane. Secondly, a pulse of 80mT and 40ns is applied to nucleate the domain wall in the ANC, followed by the WMOKE measurement. WMOKE allows to visualize the magnetization of the nanowire by subtracting the image before and after the field pulses. Finally, the pulse for DW propagation is applied and the magnetization is again evaluated by WMOKE. This was repeated for a variety of lengths and amplitudes of the pulses, as discussed in the following section.

III. RESULTS AND DISCUSSION

Fig.3 shows the results of domain wall velocity measurements. The blue line provides the DW velocity in standard pNML $[\text{Co/Pt}]_{4x}$ multilayer, while the orange line depicts the DW velocity in asymmetric Pt/Co/Ir multilayer magnetic nanowire. Fig.3 reveals significantly higher DW propagation

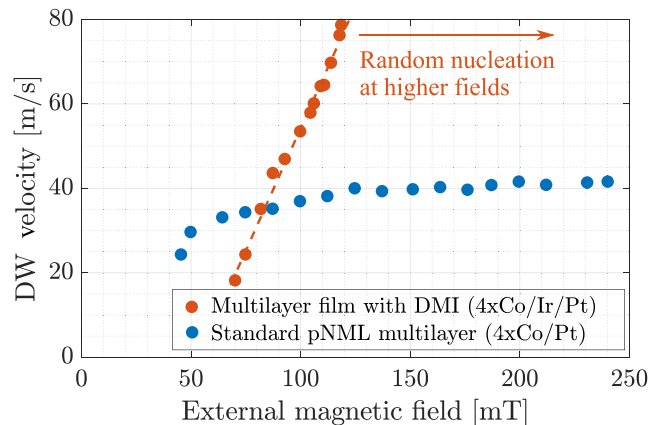


FIG. 3. Domain wall velocity in magnetic nanowires measured by wide-field Kerr-effect microscope while applying an external magnetic field of different amplitudes. The blue line shows the DW velocity in standard pNML $[\text{Co/Pt}]_{4x}$ multilayer compared to the DW velocity in DMI enhanced $[\text{Co/Ir/Pt}]_{4x}$ multilayer (orange line).

velocity (v_{DW}) in Ir enhanced Co/Pt multilayers. The maximum DW velocity in MLs with Ir reaches almost twice the maximum velocity of the nanowires without the Ir. Moreover, in Ir enhanced ML films the maximum velocity of 78m/s is reached at much lower field (120mT), while in multilayer films without Ir v_{DW} starts to saturate at around 150mT and reaches only 42m/s. Unfortunately, we were not able to measure the v_{DW} at higher than 120mT in Ir enhanced films, because for higher amplitudes massive random nucleation occurred along all over the meander structure, even if magnetic field pulse lengths are reduced to 20ns 30ns. This is quite surprising since the measurements of the magnetic anisotropy of both films provided the same values of K_{eff} . Moreover, the field pulse amplitude, required to nucleate the new DW in the ML with Ir, was 80mT, while without Ir 50ns field pulse already led to DW nucleation at the ANC. This could be due to the lack of precise control of Ga⁺ ions dose during FIB irradiation of the ANC. Probably several effects are responsible for such behavior. Especially the doubled maximal DW velocity and very small domains at demagnetized state lead to an assumption that some additional energy is playing a role in the sample with Ir.

Sandwiching the Co between two different heavy metals, preferably with large spin orbit coupling, results in Dzyaloshinskii-Moriya interaction (DMI). This is an asymmetric exchange interaction between the Co and heavy metal (here Ir). It is reported that the DW velocity v_{DW} is proportional to D/M_s .^{14,17} Where the D is the DMI constant and M_s the saturation magnetization. DMI can be interpreted as a local chiral magnetic field $\mu_0 H_{DMI}$, which points perpendicular to the DW. $\mu_0 H_{DMI}$ could be several hundredths mT as reported in Ref. 17. DMI supports the Néel DW and makes it energetically more preferable compared to the Bloch DW.¹⁸ Field driven DW wall motion can be divided into two regimes: linear and precessional. Linear DW movement occurs at low magnetic fields until the so-called Walker-breakdown field strength. Walker-breakdown is the point where a DW changes its chirality from Néel to Bloch. Increasing the driving field beyond this point leads to precessional DW movement, which also significantly reduces the DW velocity.¹⁹ Enhancing the pNML standard film stack with Ir and, therefore, inducing DMI, postpones the Walker breakdown field, and thus significantly increases velocity of DW movement by stabilizing the Néel wall configuration. Magnetic nanowires, as presented in this work, are envisioned to interconnect distant pNML logic units on the chip.²⁰ The part of the nanowire with artificial nucleation center is functioning as an input and is placed at the output of the last magnet of pNML logic unit. Such magnetic nanowire, clocked by global on-chip oscillatory magnetic field, transports the logical signal encoded in domain wall to the destination logic unit. Besides the significance for Nanomagnetic Logic, ultra-thin magnetic multilayer films with fast domain wall velocities are important for other magnetic memory and logic technologies.

IV. CONCLUSION

By enhancing the standard Co/Pt multilayer with Ir while sandwiching the cobalt layer between two different heavy metals (here Pt and Ir), we achieved significant increase of domain wall propagation velocity. Such composition of asymmetric multilayer films induces Dzyaloshinskii-Moriya interaction (DMI), which stabilizes the Néel domain wall configuration. Néel DWs can move linear w/o precession and, therefore, are much faster. Moreover, maximum DW velocity is reached at lower field amplitude, which is beneficial for pNML ultra-low power operation. These results make the pNML more competitive with *beyond CMOS* or *more-than-Moore* technologies, since the domain wall propagation is one of the most critical aspects for enabling higher clocking rates of pNML systems. Furthermore, understanding the domain wall dynamics and engineering ultra-thin magnetic films for high DW velocity is of particular interest in other magnetic logic and memory devices.

ACKNOWLEDGMENTS

The authors would like to thank the DFG (Grant Nos. SCHM 1478/9-2 and SCHM 1478/11-1) for financial support and Run Fa Jonny Qiu for MFM measurements.

¹ “The International Technology Roadmap for Semiconductors (ITRS 2.0): BEYOND CMOS,” (2015).

² M. Becherer, J. Kiermaier, S. Breitkreutz, I. Eichwald, G. Žiemys, G. Csaba, and D. Schmitt-Landsiedel, *Solid-State Electronics* **102**, 46 (2014).

- ³ I. Eichwald, S. Breitzkreutz, J. Kiermaier, G. Csaba, D. Schmitt-Landsiedel, and M. Becherer, [Journal of Applied Physics](#) **115**, 17E510 (2014).
- ⁴ I. Eichwald, S. Breitzkreutz, G. Ziemys, G. Csaba, W. Porod, and M. Becherer, [Nanotechnology](#) **25**, 335202 (2014).
- ⁵ R. P. Cowburn and M. E. Welland, [Science](#) **287**, 1466 (2000).
- ⁶ J. Hutchby, "The nanoelectronics roadmap," in *Emerging Nanoelectronic Devices* (John Wiley & Sons Ltd, 2014) pp. 1–14.
- ⁷ J. Kiermaier, S. Breitzkreutz, I. Eichwald, M. Engelstädter, X. Ju, G. Csaba, D. Schmitt-Landsiedel, and M. Becherer, [Journal of Applied Physics](#) **113**, 17B902 (2013).
- ⁸ S. Breitzkreutz, A. Fischer, S. Kaffah, S. Weigl, I. Eichwald, G. Ziemys, D. Schmitt-Landsiedel, and M. Becherer, [Journal of Applied Physics](#) **117**, 17B503 (2015).
- ⁹ J. H. Franken, M. Hoeijmakers, R. Lavrijsen, and H. J. M. Swagten, [Journal of Physics: Condensed Matter](#) **24**, 024216 (2012).
- ¹⁰ S. Breitzkreutz, J. Kiermaier, I. Eichwald, X. Ju, G. Csaba, D. Schmitt-Landsiedel, and M. Becherer, [IEEE Transactions on Magnetics](#) **48**, 4336 (2012).
- ¹¹ M. Becherer, S. Breitzkreutz, I. Eichwald, G. Ziemys, J. Kiermaier, G. Csaba, and D. Schmitt-Landsiedel, in *EUROSOL-ULIS 2015* (2015) pp. 121–124.
- ¹² B. Dieny and M. Chshiev, [Rev. Mod. Phys.](#) **89**, 025008 (2017).
- ¹³ A. Hrabec, N. A. Porter, A. Wells, M. J. Benitez, G. Burnell, S. McVitie, D. McGrouther, T. A. Moore, and C. H. Marrows, [Phys. Rev. B](#) **90**, 020402 (2014).
- ¹⁴ A. Thiaville, S. Rohart, É. Jué, V. Cros, and A. Fert, [EPL \(Europhysics Letters\)](#) **100**, 57002 (2012).
- ¹⁵ K.-W. Moon, J.-C. Lee, S.-B. Choe, and K.-H. Shin, [Review of Scientific Instruments](#) **80**, 113904 (2009).
- ¹⁶ T. R. McGuire, J. A. Aboaf, and E. Klokholm, [Journal of Applied Physics](#) **55**, 1951 (1984).
- ¹⁷ T. H. Pham, J. Vogel, J. Sampaio, M. Vaňatka, J.-C. Rojas-Sánchez, M. Bonfim, D. S. Chaves, F. Choueikani, P. Ohresser, E. Otero, A. Thiaville, and S. Pizzini, [EPL \(Europhysics Letters\)](#) **113**, 67001 (2016).
- ¹⁸ Y. Yoshimura, K.-J. Kim, T. Taniguchi, T. Tono, K. Ueda, R. Hiramatsu, T. Moriyama, K. Yamada, Y. Nakatani, and T. Ono, [Nature Physics](#) **12**, 157 (2015).
- ¹⁹ P. J. Metaxas, J. P. Jamet, A. Mougin, M. Cormier, J. Ferré, V. Baltz, B. Rodmacq, B. Dieny, and R. L. Stamps, [Phys. Rev. Lett.](#) **99**, 217208 (2007).
- ²⁰ S. Breitzkreutz, I. Eichwald, G. Ziemys, G. Hiblot, G. Csaba, D. Schmitt-Landsiedel, and M. Becherer, [Journal of Applied Physics](#) **117**, 17D507 (2015).